

Properties of Ξ^- and Ξ^0 hyperons*

C. Baltay, A. Bridgewater,† W. A. Cooper,‡ L. K. Gershwin,§
M. Habibi,|| and M. Kalelkar

Columbia University, New York, New York 10027

N. Yeh and A. Gaigalas

State University of New York at Binghamton, Binghamton, New York 13901

(Received 7 September 1973)

We report a measurement of the Ξ^- and Ξ^0 weak-decay parameters, mean lifetimes, and spins, based on 4303 Ξ^- and 652 Ξ^0 decays. We find for the Ξ^- , $\alpha = -0.376 \pm 0.038$, $\phi = 11^\circ \pm 9^\circ$, $\tau = (1.63 \pm 0.03) \times 10^{-10}$ sec, and spin equal to $\frac{1}{2}$ with higher spins excluded by more than 7 standard deviations; for the Ξ^0 , $\alpha = -0.54 \pm 0.10$, $\phi = 16^\circ \pm 17^\circ$, $\tau = (2.88_{-0.18}^{+0.21}) \times 10^{-10}$ sec, and spin equal to $\frac{1}{2}$ with higher spins excluded by more than 4 standard deviations. The results are consistent with the requirements of T invariance, and they are in fair agreement with the $\Delta I = \frac{1}{2}$ rule.

I. INTRODUCTION

We have measured the weak-decay parameters, lifetimes, and spins of the Ξ^- and Ξ^0 hyperons. The results, based on a total of 4303 $\Xi^- \rightarrow \Lambda \pi^-$ and 652 $\Xi^0 \rightarrow \Lambda \pi^0$ decays, are summarized in Table I. The Ξ 's were produced in the reactions $K^- p \rightarrow \Xi K$ and $K^- p \rightarrow \Xi K \pi$, with the incident K^- beam momentum chosen to be 1.75 GeV/ c to maximize both the two-body production cross sections and the Ξ polarizations. The average absolute polarization $\langle |P| \rangle$ was 0.42 for the Ξ^- and 0.62 for the Ξ^0 .

The spins of the Ξ^- and Ξ^0 were determined using both the Adair analysis and the Byers-Fenster method; both spins were found to be $\frac{1}{2}$. Higher spins have been excluded by 7.2 and 4.4 standard deviations for the Ξ^- and the Ξ^0 , respectively.

A spin- $\frac{1}{2}$ particle may decay to a $\Lambda \pi$ final state of either orbital angular momentum $l=0$ or $l=1$, if parity is violated in the decay. The weak-decay parameters α , β , and γ [defined below, Eqs. (6)–(8)] are a measure of the relative magnitude and phase of the amplitudes for decay to these two final states. We compare our results with the requirements of time-reversal invariance (T), charge-conjugation invariance (C), and parity conservation (P); our results are consistent with T invariance, suggest C violation, and require P violation.

The results are also compared with the predictions of the $\Delta I = \frac{1}{2}$ rule, which requires the Ξ^- and Ξ^0 decay parameters to be the same and the mean lives to be related by $\tau^0 = 2\tau^-$. We are close to agreement with these predictions, although there is a small discrepancy in the case of the lifetimes. Preliminary results of this study have been presented previously.^{1,2} This article describes our final results. A study of the $\Xi^*(1530)$ has also

been published,^{3,4} and the results of the search for rare or $\Delta S = 2$ Ξ decays will be presented in a future article.

Section II of this article describes the experimental details and the selection of events. The measurement of the weak-decay parameters is discussed in Sec. III, the lifetime measurements in Sec. IV, and the spin determinations in Sec. V. Section VI is a discussion of the results and conclusions.

II. EXPERIMENTAL DETAILS AND SELECTION OF EVENTS

The experiment was performed at the Brookhaven National Laboratory AGS using the medium-energy separated beam and the 31-in. bubble chamber filled with liquid hydrogen. A total of 860 000 photographs were taken with 23 ± 2 beam tracks each.

The beam magnets and the electrostatic separators were set to select a high-purity K^- beam of 1.75 GeV/ c , with a 1% momentum resolution. The beam was designed to separate K^- 's up to 2.9 GeV/ c ; thus the separation was very good at 1.75 GeV/ c . Figure 1 shows the separation between K^- and π^- in the beam; the π^- contamination, judging from this curve, was of the order of 1%. A careful study using δ rays⁵ produced by beamlike tracks in the bubble chamber was carried out to determine more accurately the non- K^- contamination in the beam. The results of this study are shown in Fig. 2. The sum of the π^- and μ^- contamination was $(1.03 \pm 0.19)\%$. The relative π^- and μ^- content of this contamination was estimated by measuring the interaction cross section of the " π or μ " tracks (beam tracks with large δ rays). This led to an estimate of $(0.50 \pm 0.25)\%$ for the π^- contamination.

It was important to keep the π^- contamination as

TABLE I. Summary of final results.

	α	ϕ	β	γ	τ (10^{-10} sec)	Spin
Ξ^-	-0.376 ± 0.038	$(11 \pm 9)^\circ$	0.18 ± 0.14	$0.91^{+0.015}_{-0.040}$	1.63 ± 0.03	$\frac{1}{2}$
Ξ^0	-0.54 ± 0.10	$(16 \pm 17)^\circ$	0.23 ± 0.24	$0.81^{+0.03}_{-0.10}$	$2.88^{+0.21}_{-0.19}$	$\frac{1}{2}$

small as possible since some of the previous Ξ experiments had a problem with $\pi^-p \rightarrow \Lambda K^0$, $\Sigma^0 K^0$, or $\Lambda K^0 \pi^0$ events, which were a background in the $K^-p \rightarrow \Xi^0 K^0$ sample. To measure this background, we took 1.2% of our total exposure with a pure π^- incident beam. These π^- pictures were then scanned for $K^-p \rightarrow \Xi^0 K^0$ candidates just like the K^- film; only three events in the entire π^- film were ambiguous with Ξ^0 events. Thus, we estimate that only ≤ 1 of our 652 Ξ^0 events was due to π^- background.

The reactions in which the Ξ 's were produced are the following. (The number of events in each case is given in square brackets.)

$$K^-p \rightarrow \Xi^- K^+ \quad [2702], \quad (1)$$

$$- \Xi^- K^+ \pi^0 \quad [498], \quad (2)$$

$$- \Xi^- K^0 \pi^+ \quad [1103], \quad (3)$$

$$- \Xi^0 K^0 \quad [443], \quad (4)$$

$$- \Xi^0 K^+ \pi^- \quad [209]. \quad (5)$$

The Ξ^- events that were used all had the topology of a two-prong with a kink on the negative track (the Ξ^- decay) with a visible $\Lambda \rightarrow p\pi^-$ decay. The $\Xi^0 K^0$ events were required to have both the $K^0 \rightarrow \pi^+ \pi^-$ and $\Lambda \rightarrow p\pi^-$ decays visible, and thus had the topology of a zero-prong with two vees, one of which did not necessarily point to the zero-prong end point since it was a Λ from Ξ^0 decay. In the

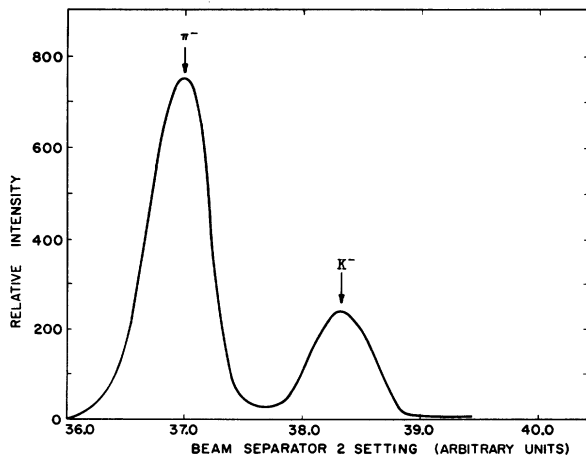


FIG. 1. The K^- and π^- separation at 1.75 GeV/c in the beam to the 31-in. chamber at Brookhaven National Laboratory, using two stages of electrostatic beam separators.

case of the $\Xi^0 K^+ \pi^-$ events, the regular scan only accepted candidates in which the K^+ decay was visible. These had the topology of a two-prong with a kink in the positive track and a vee (possibly not pointing to the two-prong vertex). An additional sample comprising 145 of the 209 events of $\Xi^0 K^+ \pi^-$ was obtained from a separate experiment studying two-prongs with vees.⁶ That experiment scanned only about half the film for the topology of two-prong plus a (possibly nonpointing) vee. The 145 events were obtained by fitting the two-prongs with vees to the hypothesis $\Xi^0 K^+ \pi^-$. (These events are discussed further in Sec. III B.)

Obvious electron pairs were disregarded during the scan. However, the scan rules were such that if there were any possibility of an event's being a Ξ event, it was recorded and measured. About 13 000 candidates were measured on conventional film plane digitizers and processed through the geometrical reconstruction and kinematic fitting programs TVGP and SQUAW. Failures were examined by a physicist and remeasured when necessary.

Partly because of the relatively low beam momentum and the high (22.4 kG) magnetic field, there were no serious ambiguities in the interpretation of the fits. As discussed above, there was

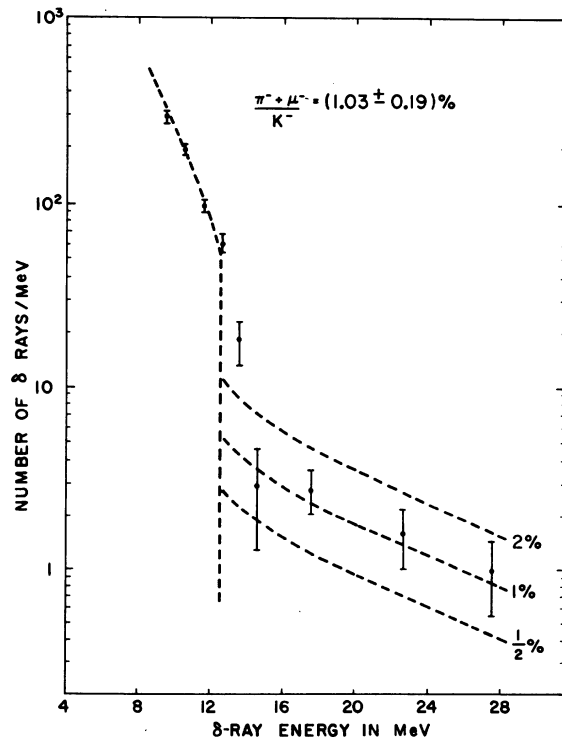


FIG. 2. Energy spectrum of δ rays produced by beamlike tracks in the chamber. The maximum energy for δ rays produced by 1.75-GeV/c K^- was 12.4 MeV.

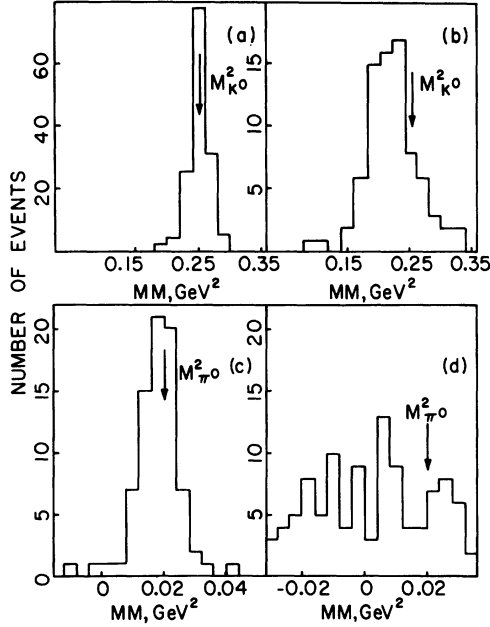


FIG. 3. Square of the mass of the missing neutral particle (a) for $\Xi^- \pi^+ (K^0)$ events, assigning a π^+ mass to the positive track; (b) for $\Xi^- K^+ (\pi^0)$ events, assigning a π^+ mass to the positive track; (c) for $\Xi^- K^+ (\pi^0)$ events, assigning a K^+ mass to the positive track; and (d) for $\Xi^- \pi^+ (K^0)$ events, assigning a K^+ mass to the positive track.

no problem with π^- contamination in the beam. The only ambiguities were between the $\Xi^- K^+ \pi^0$ and $\Xi^- \pi^+ K^0$ final states. Of the ~ 1600 events in these two final states, about 200 were ambiguous. These were resolved by using the bubble density information on the positive track. This was possible since the momentum of the positive track varied between 200 and 500 MeV/c; thus the bubble densities, when this track was interpreted as a K^+ , were at least twice the bubble density of the track interpreted as a π^+ . To check the reliability of this procedure, the missing-mass distributions of both final states, interpreting the positive track as both a π^+ and a K^+ , were examined. As can be seen in Fig. 3, the $\Xi^- K^+ \pi^0$ events show no peak at the K^0 mass when the positive track is called a π^+ , and the converse is true for the $\Xi^- \pi^+ K^0$ events.⁶ At the end of the analysis, we felt that the number of misidentified or fake events in the Ξ^- and Ξ^0 samples was less than $\sim 1\%$.

The numbers of events satisfying the final selection criteria for the various final states are shown in Eqs. (1)–(5).

III. DECAY PARAMETERS

In the decay $\Xi^- \rightarrow \Lambda \pi$, both parity-conserving and parity-changing amplitudes are allowed. Let these

amplitudes be A_p and A_s , respectively. Then the decay parameters are given by

$$\alpha_{\Xi} = \frac{2 \operatorname{Re}(A_s^* A_p)}{|A_s|^2 + |A_p|^2}, \quad (6)$$

$$\beta_{\Xi} = \frac{2 \operatorname{Im}(A_s^* A_p)}{|A_s|^2 + |A_p|^2}, \quad (7)$$

$$\gamma_{\Xi} = \frac{|A_s|^2 - |A_p|^2}{|A_s|^2 + |A_p|^2}. \quad (8)$$

We have measured the Ξ spin to be $\frac{1}{2}$, as discussed in Sec. V of this article. Then the joint decay distribution for $\Xi^- \rightarrow \Lambda \pi$, $\Lambda \rightarrow p \pi$ is given by

$$I = 1 + \alpha_{\Xi} \vec{P}_{\Xi} \cdot \hat{\Lambda} + \alpha_{\Lambda} \hat{p} \cdot [(\alpha_{\Xi} + \vec{P}_{\Xi} \cdot \hat{\Lambda}) \hat{\Lambda} + \beta_{\Xi} (\vec{P}_{\Xi} \times \hat{\Lambda}) + \gamma_{\Xi} \hat{\Lambda} \times (\vec{p} \times \hat{\Lambda})], \quad (9)$$

where \vec{P}_{Ξ} = Ξ polarization vector, $\hat{\Lambda}$ = Λ direction in the Ξ rest frame (unit vector), and \hat{p} = proton direction in Λ rest frame (unit vector).

An alternate form is obtained by defining

$$\begin{aligned} \hat{z} &= \hat{\Lambda}, \\ \hat{x} &= (\vec{P}_{\Xi} \times \hat{\Lambda}) / (|\vec{P}_{\Xi} \times \hat{\Lambda}|), \\ \hat{y} &= \hat{z} \times \hat{x}, \end{aligned} \quad (10)$$

$$\cos \chi = (\vec{P}_{\Xi} \cdot \hat{\Lambda}) / |\vec{P}_{\Xi}|:$$

$$\begin{aligned} I &= 1 + \alpha_{\Xi} P_{\Xi} \cos \chi \\ &+ \alpha_{\Lambda} [(\alpha_{\Xi} + P_{\Xi} \cos \chi) \hat{p} \cdot \hat{z} \\ &+ \beta_{\Xi} P_{\Xi} \sin \chi \hat{p} \cdot \hat{x} + \gamma_{\Xi} P_{\Xi} \sin \chi \hat{p} \cdot \hat{y}]. \end{aligned}$$

A. α_{Ξ^-}

If the coordinate system in Eq. (10) is changed to a polar coordinate system with the same z axis and the distribution is integrated over the azimuthal angle, the terms dependent on β_{Ξ} and γ_{Ξ} vanish. The resulting distribution is

$$I' = 1 + \alpha_{\Xi} \vec{P}_{\Xi} \cdot \hat{\Lambda} + \alpha_{\Lambda} \hat{p} \cdot (\alpha_{\Xi} + \vec{P}_{\Xi} \cdot \hat{\Lambda}) \hat{\Lambda}. \quad (11)$$

If the direction of the production normal is integrated over, i.e., the Ξ polarization information is not used, the distribution becomes

$$I'' = 1 + \alpha_{\Lambda} \alpha_{\Xi} \hat{p} \cdot \hat{\Lambda}. \quad (12)$$

Using the events from the two-body production reaction (1), a likelihood based on the probability distribution (11) was maximized for both α_{Ξ^-} and the polarizations. Twenty bins, corresponding to twenty equal intervals in $\hat{K}^- \cdot \hat{K}^+$ (where \hat{K}^- and \hat{K}^+ are unit vectors along the incident K^- and outgoing K^+ , respectively), as evaluated in the production c.m. system, were used to determine the polarizations. The above expression was then used in a maximum-likelihood analysis for the 21 parameters. The value $\alpha_{\Lambda} = 0.645$ was used.

To simplify this analysis, an iterative method was used. First α_{Ξ} was evaluated using the $\alpha_{\Lambda}\alpha_{\Xi}$ term of Eq. (12), which is independent of the Ξ polarization. For the two-body events, this gave $\alpha_{\Xi} = -0.36 \pm 0.06$. This value of α was used to evaluate the Ξ polarization in each of the 20 bins, using Eq. (11). Then these polarizations were used to find a new value for α_{Ξ} . The procedure rapidly converged to $\alpha_{\Xi} = -0.377 \pm 0.048$ and the 20 bin polarizations shown in Fig. 4.

Next, we fitted the production angular distribution (summed over the azimuthal angle) to Legendre polynomials, and the polarization times the angular distribution to associated Legendre polynomials:

$$\frac{d\sigma}{d(\cos\theta)} = \sum_{l=0}^7 a_l P_l(\cos\theta), \quad (13)$$

$$P_{\Xi} \frac{d\sigma}{d(\cos\theta)} = \sum_{l=1}^7 b_l P_l^1(\cos\theta), \quad (14)$$

with $\cos\theta = \hat{K}^- \cdot \hat{K}^+$.

The angular distribution and the result of the fit to Eq. (13) are shown in Fig. 5.

Since α_{Ξ} was used to evaluate the polarization in performing this fit, the procedure was again iterated. The parameter α_{Ξ} was calculated by using the polarization given by the ratio of $P_{\Xi}[d\sigma/d(\cos\theta)]$ to $d\sigma/d(\cos\theta)$ at the appropriate value of $\cos\theta$. The final result of the iteration, based on 2123 events, was $\alpha = -0.379 \pm 0.045$. (This error includes the effect of uncertainty in the polarizations in the calculation of α .) The polarization obtained from the ratio of $P_{\Xi}[d\sigma/d(\cos\theta)]$ to $d\sigma/d(\cos\theta)$ is shown by the curve in Fig. 4. The coefficients of the polynomials of Eqs. (13) and (14) from these fits are given in Table II.

There were several corrections that were made

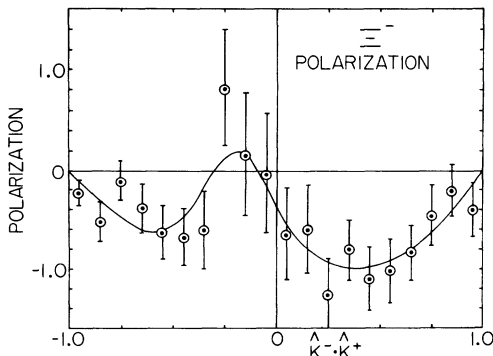


FIG. 4. Polarization of the Ξ^- in the reaction $K^- + p \rightarrow \Xi^- + K^+$ as a function of the Ξ^- production angle. Note that the forward-produced Ξ^- are near $\hat{K}^- \cdot \hat{K}^+ = -1.0$ in this distribution. The solid line is the fit described in the text.

TABLE II. Coefficients of the associated Legendre polynomials of Eqs. (13) and (14) obtained in the fit to the angular distributions and polarizations in the reactions $K^- + p \rightarrow \Xi^- + K^+$ and $K^- + p \rightarrow \Xi^0 + K^0$. The coefficients have been normalized such that $a_1 = 1.0$.

l	Ξ^-		Ξ^0	
	a_l	b_l	a_l	b_l
1	1.000 ± 0.028	0.000 ± 0.707	1.000 ± 0.069	0.000 ± 0.707
2	-0.421 ± 0.037	0.472 ± 0.074	-0.218 ± 0.086	-0.370 ± 0.211
3	0.637 ± 0.037	0.139 ± 0.096	0.660 ± 0.080	0.887 ± 0.275
4	-0.429 ± 0.036	0.259 ± 0.106	0.098 ± 0.076	-0.172 ± 0.293
5	0.116 ± 0.035	-0.213 ± 0.116	0.082 ± 0.081	0.648 ± 0.272
6	-0.042 ± 0.033	-0.026 ± 0.121	0.195 ± 0.081	0.005 ± 0.271
7	0.061 ± 0.032	-0.0168 ± 0.121	-0.011 ± 0.077	-0.225 ± 0.294

to obtain this value of α . The following sections describe those effects that were studied, and the corrections made.

1. Slow π^- from Λ decay and small Λ opening angle

There are a few possible systematic losses which have a direct effect on α_{Ξ} . An example is the loss of slow π^- tracks from $\Lambda \rightarrow p\pi^-$ decays. If the π^- momentum is less than 50 MeV/c, it will have a range of less than 3 cm, and if the track is not seen, the remaining proton will look like a proton recoil, produced by a scattering neutron. This loss is most important for Λ 's with momenta about 800 MeV/c, where a π^- emitted backward in the Λ rest frame can be very slow in the laboratory. The Ξ momentum spectrum is such that more 800-MeV/c Λ 's result from Ξ decays with the Λ emitted backward in the Ξ rest frame than with the Λ forward. Thus, the loss of slow π^- events would mean the loss of protons going in the opposite direction from the Λ polarization, resulting in a bias making the apparent α of the remaining events

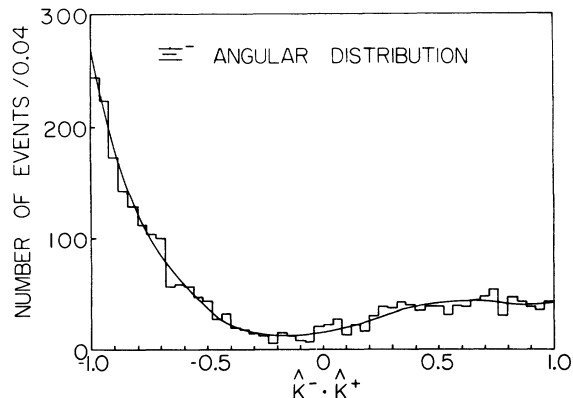


FIG. 5. Angular distribution of the Ξ^- in the center-of-mass system for the reaction $K^- + p \rightarrow \Xi^- + K^+$. Note that the forward-produced Ξ^- are near $\hat{K}^- \cdot \hat{K}^+ = -1.0$ in this distribution.

too positive. (The effect of this depends on the Ξ momentum spectrum.)

A similar bias would result from the loss of slow protons. However, the slowest proton that can result from the reaction $K^-p \rightarrow \Xi^-K^+$, $\Xi^- \rightarrow \Lambda\pi^-$, $\Lambda \rightarrow p\pi$ is about 300 MeV/c for our beam momentum, so no loss should occur. (This corresponds to a range of about 15 cm for a proton.)

Another possible loss is the loss of small opening-angle Λ decays. Because at high momenta these look like electron pairs from γ conversions, the scanners might have a poorer efficiency for finding such events than for larger opening-angle events. The fastest Λ 's come from Λ 's forward in the Ξ decay. Small-opening-angle decays result more frequently from backward protons than from forward ones, so this loss might mean a bias in α_x toward positive values.

To guard against all these losses, a means of making an unbiased cut was used. This relied on the fact that the parameters being measured depend on a scalar product, e.g., $\hat{p} \cdot \hat{\Lambda}$ for α_x . A likelihood function is still valid if two regions in $\hat{p} \cdot \hat{\Lambda}$ are omitted which are related by an inversion through the origin. Then the omitted region will not affect the validity or normalization of the likelihood function.

To make the cut against slow π^- events, first all events with π^- momentum less than 50 MeV/c were omitted. Then, the Λ decay products were transformed to the Λ rest frame, the proton and π^- momenta were interchanged, and the event was transformed back to the lab. If the new π^- momentum

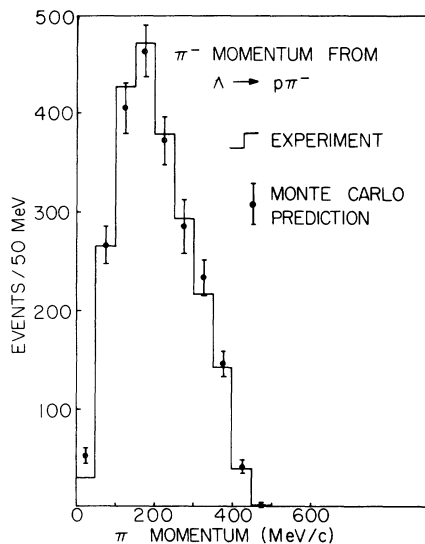


FIG. 6. Momentum distribution of the π^- from the $\Lambda \rightarrow p + \pi^-$ decay for Λ 's produced in the $\Xi^- \rightarrow \Lambda + \pi^-$ decays, compared with the results of a Monte Carlo calculation.

became less than 50 MeV/c, the event was removed. Thus, the cut was symmetrical in the Λ rest frame.

To check for losses such as these, a Monte Carlo program was used. The actual Λ events were used, but they were allowed to decay randomly in the Λ c.m. system, with the decay distribution corresponding to the final values of α_x . Figure 6 shows the π^- momentum spectrum compared to this Monte Carlo calculation. The loss of π^- tracks below 50 MeV/c is evident; the loss represents about 1.5% of all events.

The projected opening-angle distribution for the $\Lambda \rightarrow p + \pi^-$ decays, compared with the Monte Carlo, is shown in Fig. 7. There is an indication of a small loss of events at small opening angles. (This is more pronounced if the distribution is made for only high-momentum Λ 's.) To protect against biases due to such losses, the π^- momentum cut was increased to 100 MeV/c for Ξ^- 's with momentum above 1250 MeV/c in the lab. This had the effect of cutting out the small-opening-angle Λ 's; for a Λ momentum of 1500 MeV/c, this corresponds to a 10° opening-angle cut.

The correction in α_x due to this cut was -0.012 ; about 10% of the events were removed.

2. Small kink loss

For small kinks in the decay $\Xi^- \rightarrow \Lambda\pi^-$, the events become hard to identify. This is obvious in Fig. 8, which shows the size of the $\Xi^- \rightarrow \pi^-$ kink compared to the Monte Carlo prediction. To check for biases in the lost events, α_x was evaluated for the events where the projected kink angle was less than 0.3 rad. This region gave $\alpha = -0.45 \pm 0.09$

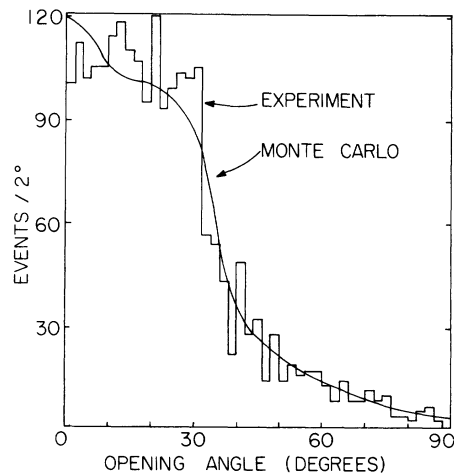


FIG. 7. Distribution in the opening angle (the angle between the p and the π^- in the laboratory frame) for Λ decays for Λ 's produced in the $\Xi^- \rightarrow \Lambda + \pi^-$ decays, compared with the results of a Monte Carlo calculation.

based on about $\frac{1}{3}$ of all events, and so was consistent with the rest of the sample.

The asymmetry in the Ξ decay depends on the polarization, which is perpendicular to the production plane. A bias in the production plane, such as results from the bias against small kinks, does not affect our evaluation of polarizations or of the decay parameters.

3. Scanning checks

About $\frac{1}{3}$ of the film was double-scanned, and the rolls chosen for second scanning were scattered throughout the exposure. The over-all single-scan efficiency was found to be 84% for reaction (1) and 80% for reaction (4).

The efficiency varied with Ξ^- momentum from 90% for the slowest to 75% for the fastest Ξ^- . The possibility that the loss was biased with respect to α was investigated extensively; for example, by dividing the events into different $(\hat{\Lambda} \cdot \hat{p})$ regions, correlating these regions with laboratory topologies, and evaluating the scan efficiency for those topologies.

Most systematic effects in the laboratory (position in the chamber, right-left effects, etc.) do not result in biases in the Λ rest frame. However, a correlation between the Ξ decay direction and the Λ decay direction may lead to a bias. For example, consider events in which the Λ from Ξ decay goes to the left of the Ξ direction (as seen in the chamber looking downstream) and the proton from the Λ decay goes to the left of the Λ direction. The Λ polarization is longitudinal in the Ξ rest frame. In the laboratory, it is rotated relative to the Ξ direction. This transverse component causes these events to fill a particular region in the

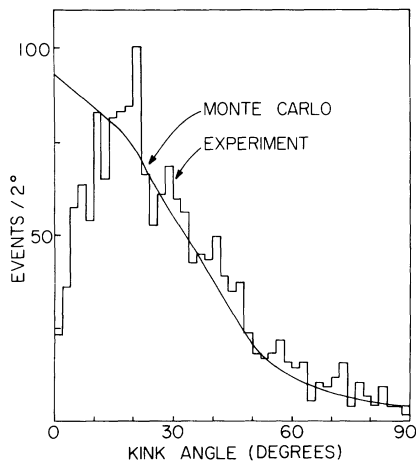


FIG. 8. Distribution in the kink angle (the angle between the Ξ^- and the π^-) in the decays $\Xi^- \rightarrow \Lambda + \pi^-$, compared with the results of a Monte Carlo calculation.

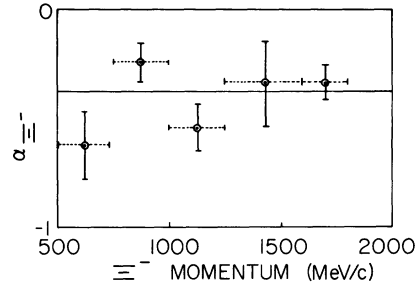


FIG. 9. The results for the determination of α_{Ξ^-} as a function of the Ξ^- momentum.

$(\hat{\Lambda} \cdot \hat{p})$ distribution, since $\hat{\Lambda}$ is measured in the Ξ rest frame. Thus, the loss of these events may result in a bias.

Because the efficiency for this category (where the Ξ^- momentum was greater than 1250 MeV/c) was $(72 \pm 5)\%$ vs $(81 \pm 3)\%$ for the remainder, the events were weighted by the inverse of their scan efficiencies in the four regions characterized by $\Xi^- - \pi^-$ kink to right or left and $\Lambda - p$ decay to right or left. This changed α by -0.028 ± 0.018 .

A plot of α vs Ξ^- momentum is shown in Fig. 9. There is no evidence of a bias at high momentum from this plot, even though the scan efficiency is worse at high momentum.

4. Length of Ξ or Λ track

Figures 10 and 11 show the Ξ^- and Λ decay-length distributions, compared to a Monte Carlo calculation based on the momentum spectrum of true events. The experimental Ξ^- length distribution is weighted by the inverse of the detection probability for the Λ , so that the Ξ^- decay and

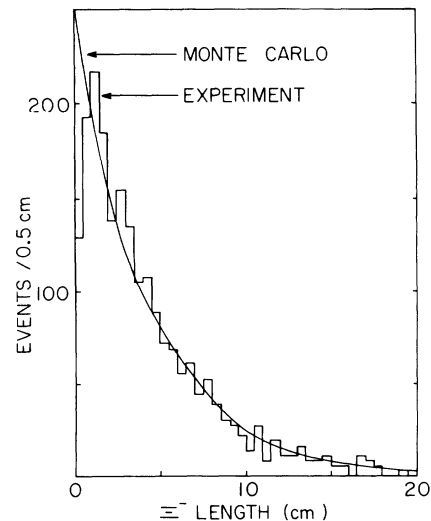


FIG. 10. Distribution in the Ξ^- length, compared with the Monte Carlo calculation.

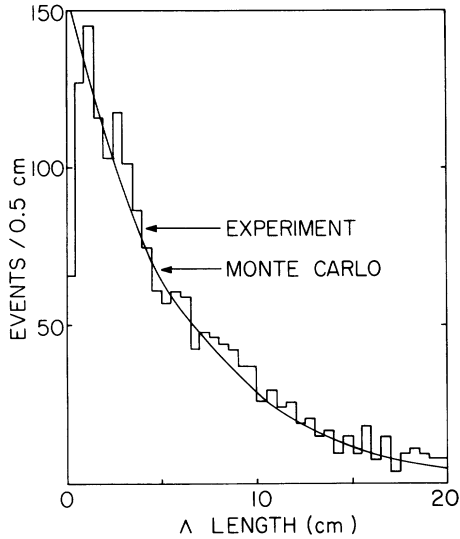


FIG. 11. Distribution in the Λ^0 length for Λ 's produced in the decay $\Xi^- \rightarrow \Lambda + \pi^-$, compared with the Monte Carlo calculation.

geometrical efficiency determine the distribution. There is apparently a loss in the first two bins of each distribution. To show that the bias due to this loss is negligible, we calculated α from the $l_{\Xi} < 1$ cm events and the $l_{\Lambda} < 1$ cm events. The results were $\alpha = -0.56 \pm 0.12$ for Ξ lengths less than 1 cm and -0.36 ± 0.15 for Λ lengths less than 1 cm.

5. Three-body events

For reactions (2) and (3), the term in Eq. (12) involving $\alpha_{\Xi}\alpha_{\Lambda}$ may be used in a likelihood calculation. This gives a value of $\alpha_{\Xi} = -0.41 \pm 0.08$, which is independent of the Ξ polarization.

It is also possible to evaluate polarizations for these events, and iterate as was done for the two-body events. A net polarization was found in the $\hat{K}^- \times \hat{\Xi}^-$ direction, and this was used in an iterative procedure as before to obtain $\alpha_{\Xi} = -0.37 \pm 0.07$.

The analysis procedures used for the three-body

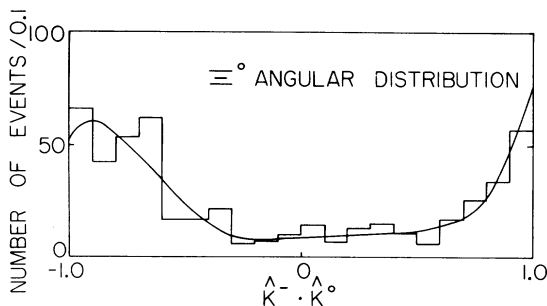


FIG. 12. Angular distribution of the Ξ^0 in the center-of-mass system for the reaction $K^- + p \rightarrow \Xi^0 + K^0$. Note that the forward-produced Ξ^0 are near $\hat{K}^- \cdot \hat{K}^0 = -1.0$ in this distribution.

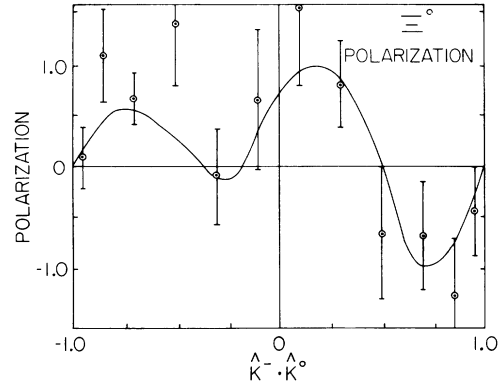


FIG. 13. Polarization of the Ξ^0 in the reaction $K^- + p \rightarrow \Xi^0 + K^0$ as a function of the Ξ^0 production angle. Note that the forward-produced Ξ^0 are near $\hat{K}^- \cdot \hat{K}^0 = -1.0$ in this distribution. The solid line is the fit described in the text.

events were the same as the procedures described above for the two-body events. A careful evaluation of possible biases was carried out in the same way as discussed in Secs. III A 1-4 above. The corrections due to these effects, which were all essentially negligible, have been included in the result $\alpha_{\Xi} = -0.37 \pm 0.07$ quoted above.

6. Final result for α_{Ξ^-}

The result of combining the 2123 two-body and the 1313 three-body events is

$$\alpha_{\Xi^-} = -0.376 \pm 0.038. \quad (15)$$

B. α_{Ξ^0}

The analysis was similar to that for the Ξ^- parameter. In both, a fiducial volume was imposed which was about 5 cm smaller than the chamber. This was important in the case of Ξ^0 's especially because the unseen decay vertex of the Ξ^0 makes the fit less constrained than the Ξ^- case. The events outside this volume were found to have an α value of -0.20 ± 0.20 , quite different from the rest of the sample. (Further reducing the fiducial volume cut did not appreciably alter the result.)

There were 443 events of the reaction



Of these, 129 were omitted because either the production point, the Λ decay point, or the K^0 decay point was outside the fiducial volume.

The correction for slow π^- events was made as in the Ξ^- case, and a similar correction was made for small-opening-angle events. However, since the small-opening-angle Λ would be confused with

an e^+e^- pair only if it pointed to the production point, the opening-angle correction was made only for those Λ 's pointing within 2° of the production point. When these corrections were made, there was no change in the value of α .

The angular distribution for the reaction (4) is shown in Fig. 12, and the polarization of the $\Xi^{0\prime}$ s is shown in Fig. 13. The coefficients of the Legendre polynomials of Eqs. (13) and (14) from the fit to the two-body Ξ^0 events are given in Table II.

The α value obtained from the two-body production reaction (4) was $\alpha = -0.59 \pm 0.11$. (The error quoted includes the effects of uncertainties in the polarizations.) The value obtained from the $\alpha_{\Xi}\alpha_{\Lambda}$ term only [Eq. (12)], ignoring polarizations, was -0.68 ± 0.16 .

An additional 64 events fitting $\Xi^0 K^+ \pi^-$ were found, where the K^+ track stopped and decayed in the chamber. These events were analyzed in the same fashion as the three-body Ξ^- events. Of these, 46 survived the fiducial volume cuts, and these gave a value of $\alpha = -0.68 \pm 0.16$.

A separate scan studied events of the topology two-prong plus vee. This scan found 179 events fitting $\Xi^0 K^+ \pi^-$ with a visible Λ decay. Of these, 76 also made fits to $K^- + p \rightarrow \Lambda^0 + \pi^+ + \pi^- + (x^0)$, where the missing mass (of x^0) was consistent with one or two π^0 's.

The ambiguous events were resolved by examining the ionization of the positive prong at the production vertex. This track was a K^+ if the reaction was $K^- p \rightarrow \Xi^0 K^+ \pi^-$, and a π^+ otherwise. In about 80% of the cases, the ionization provided a clear means of resolving the ambiguity. In the remaining 20% a guess was made, and the effect of including or excluding these events was studied and included in our final error. We excluded 34 events, leaving a sample of 145 events, yielding $\alpha = -0.38 \pm 0.19$.

The average value, combining all three samples (505 events) is

$$\alpha_{\Xi^0} = -0.54 \pm 0.10. \quad (16)$$

C. ϕ_{Ξ^-}

To incorporate the constraint $\alpha^2 + \beta^2 + \gamma^2 = 1$, let $\beta = \sin\phi \sqrt{1 - \alpha^2}$ and $\gamma = \cos\phi \sqrt{1 - \alpha^2}$. Then the error in ϕ is more nearly Gaussian than the errors in β or γ . The likelihood expression based on Eq. (9) was maximized for the best value of ϕ . Only events from the two-body reaction (1) were used in this analysis. The polarizations, selection criteria, and weighting described in the Ξ^- analysis for α were used. The result based on 2123 events was

$$\phi_{\Xi^-} = +11^\circ \pm 9^\circ \quad (17)$$

giving

$$\beta_{\Xi^-} = 0.18 \pm 0.14 \text{ and } \gamma_{\Xi^-} = 0.91_{-0.04}^{+0.015}. \quad (18)$$

The errors above include the uncertainty in the Ξ polarization.

D. ϕ_{Ξ^0}

Using the Ξ^0 events from reaction (4) only and the polarizations as in Fig. 13, we find, from a sample of 314 events,

$$\phi_{\Xi^0} = +16^\circ \pm 17^\circ \quad (19)$$

giving

$$\beta_{\Xi^0} = 0.23 \pm 0.24 \text{ and } \gamma_{\Xi^0} = 0.81_{-0.10}^{+0.08}. \quad (20)$$

The errors again include the uncertainties in the Ξ polarization.

A series of checks for possible systematic effects on ϕ failed to reveal any dependence on topology, length of Ξ track, scanner, or Ξ momentum for either the Ξ^- or Ξ^0 decays.

IV. LIFETIMES

The normalized probability for an event to decay at a proper time t , when it has a mean life τ , is

$$P(t, \tau) = \frac{e^{-t/\tau}}{\tau(e^{-t_{\min}/\tau} - e^{-t_{\max}/\tau})}, \quad (21)$$

where t_{\min} and t_{\max} are the minimum and maximum proper times observable, respectively.

There are two complications. The first is that the Ξ^- loses energy in passing through hydrogen. To get t , a momentum loss of $(0.25 \text{ MeV}/c)/\beta^2$ per cm was used to correct for energy loss. (The correction was minor.)

The second complication is that the detection of the Ξ decay depends on detection of the Λ decay. A Ξ decaying near the side wall of the chamber is less likely to be detected than one near the center because of the decreased probability of observing the Λ decay. Two methods of analysis were used to correct for this effect. One is essentially that described in Ref. 7. The probability that an event occurs with Ξ proper time t_1 and Λ proper time t_2 is

$$P(t_1 t_2 \tau_1 \tau_2) = n e^{-t_1/\tau_1} e^{-t_2/\tau_2}, \quad (22)$$

where $\tau_1 = \Xi$ mean life and $\tau_2 = \Lambda$ mean life. The factor n is a normalization factor, chosen to give unit probability for detecting an event in the fiducial volume. This normalization was evaluated by a two-dimensional numerical integration. For each Ξ decay point in the integration, the Λ decay direction was kept the same as the real event direction, and the potential path length was found for

the Λ . The resulting normalized probability was used in a maximum-likelihood calculation for the Ξ mean life using a Λ mean life of 2.51×10^{-10} sec.

In the case of the Ξ^0 , the decay point was not observed and had to be calculated from the fitted angles. To account for this, a Gaussian error function G was included in the probability:

$$P'(t_1, t_2, \tau_1, \tau_2) = \int_0^{t_2} dx G(x, l) P(t_1'(x), t_2'(x), \tau_1, \tau_2), \quad (23)$$

where

$$G(x, l) = \frac{1}{\sqrt{2\pi} \sigma} e^{-(x-l)^2/2\sigma^2};$$

$l = \Xi^0$ length,

$\sigma =$ error in Ξ^0 length,

$l_J =$ sum of Ξ^0 and Λ lengths,

$t_1'(x) =$ proper time for Ξ^0 ,
assuming Ξ^0 length x ,

$t_2'(x) =$ proper time for Λ ,
assuming Ξ^0 length x .

Minimum lengths of 0.75 cm for the Ξ^- and 0.5 cm for the Λ^0 were required for the Ξ^- lifetime calculation. For the Ξ^0 , the joint $\Xi^0 + \Lambda^0$ length was required to be >0.5 cm. The joint $\Xi^0 - \Lambda^0$ length is the distance of the Λ decay point from the Ξ production vertex. The maximum length allowed was determined by a fiducial volume approximately 5 cm from the edges of the chamber. After these length cuts, a sample of about 3100 Ξ^- and 392 Ξ^0 decays remained. This procedure gave mean life values of $\tau_{\Xi^-} = (1.62 \pm 0.04) \times 10^{-10}$ sec for the Ξ^- and $\tau_{\Xi^0} = (2.85_{-0.18}^{+0.20}) \times 10^{-10}$ sec for the Ξ^0 .

An alternate procedure is to consider the Ξ decay as given by an ordinary lifetime likelihood function, Eq. (21). Then the detection problem is taken into account by weighting the contribution of each event to the likelihood by the inverse of the Λ detection probability. The resulting likelihood is the same as if all Λ 's were detected (except for the problem of finding the statistical error). This procedure gave a Ξ^- mean life of

$$\tau_{\Xi^-} = (1.63 \pm 0.03) \times 10^{-10} \text{ sec}, \quad (24)$$

with an average Λ weight of 1.3.

In the case of the Ξ^0 , this method was used only for events for which the projected laboratory angle between the Ξ^0 and Λ^0 was greater than 0.02 rad, since events more collinear than this had large Ξ^0 length errors. The 281 events inside the fiducial volume which satisfy this collinearity test gave a mean life of $(2.82 \pm 0.20) \times 10^{-10}$ sec. For another 111 events, a likelihood calculation was used

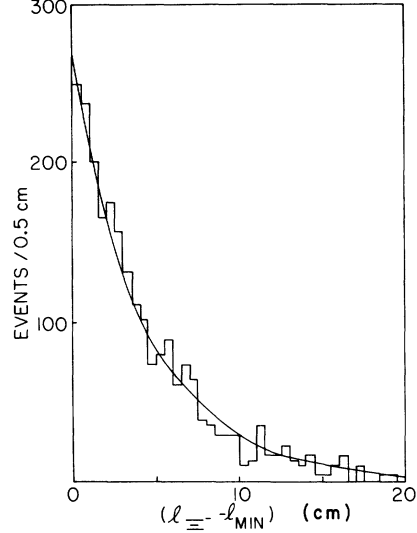


FIG. 14. Distribution in $(l_{\Xi^-} - l_{\min})$, where l_{Ξ^-} is the Ξ^- length and $l_{\min} = 0.75$ cm. The curve represents the distribution expected for the Ξ^- mean life obtained from the maximum-likelihood analysis.

which depended only on the joint $\Xi^0 - \Lambda$ length and not on the location of the decay point. These events gave the mean life value of $(3.09 \pm 0.46) \times 10^{-10}$ sec. The effect of the length error on this procedure was evaluated by smearing the lengths of the real events by their errors and recalculating the lifetime. This procedure shifted the mean life an average of 0.04×10^{-10} sec higher, so the value of 2.82×10^{-10} sec was corrected to 2.78×10^{-10} sec.

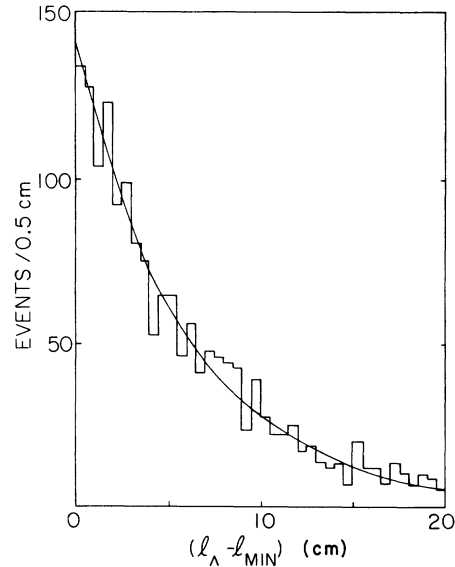


FIG. 15. Distribution in $(l_{\Lambda} - l_{\min})$, where l_{Λ} is the Λ length for the $\Xi^- \rightarrow \Lambda + \pi^-$ decay, and $l_{\min} = 0.5$ cm. The curve represents the distribution expected for a Λ mean life of 2.51×10^{-10} sec.

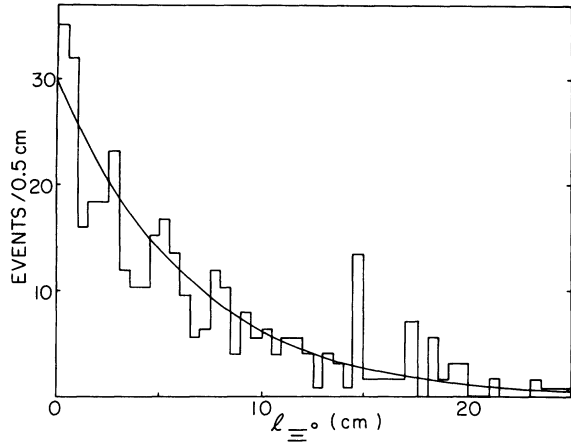


FIG. 16. Distribution in the Ξ^0 length. The curve represents the distribution expected for the Ξ^0 mean life obtained from the maximum-likelihood analysis.

The effect of the scan efficiency (which was lower for the longest events) was to change the mean life by -0.06 ± 0.06 . This required a correction of $+0.06 \pm 0.06$ to the lifetime result. When these corrections were applied and the results of the two samples were combined, we obtained the final value

$$\tau_{\Xi^0} = (2.88_{-0.19}^{+0.21}) \times 10^{-10} \text{ sec.} \quad (25)$$

The Ξ^- and Ξ^0 lifetimes were not sensitive to the Λ lifetime assumed. Changing the Λ mean life by 10% only changes the Ξ mean life by 0.5%. Other systematic uncertainties such as mass values, magnetic field normalization, and the effect of measurement errors have negligible effect on the lifetime results.

Figures 14–17 show comparisons of the lengths

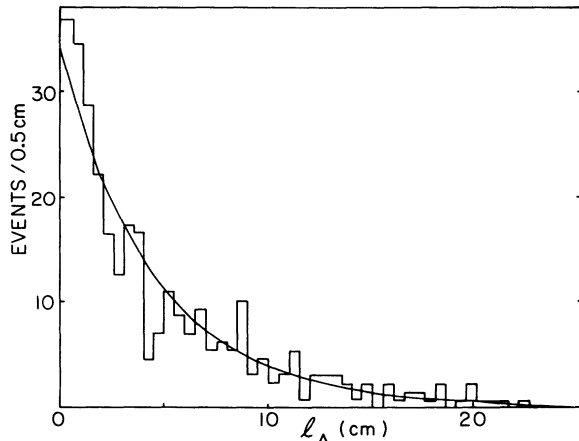


FIG. 17. Distribution in the Λ^0 length for Λ 's from the decay $\Xi^0 \rightarrow \Lambda^0 + \pi^0$. The curve represents the distribution expected for a Λ mean life of 2.51×10^{-10} sec.

of the Ξ and Λ tracks with Monte Carlo predictions based on these lifetimes. In the case of the Ξ^- , the minimum length cut has been subtracted before plotting.

V. DETERMINATION OF THE Ξ^- AND Ξ^0 SPINS

We used both the Adair analysis⁸ and the Byers-Fenster method⁹ to determine the spins. The Adair analysis requires Ξ 's produced near the incident K^- direction, while the Byers-Fenster technique requires that the Ξ 's be polarized. Since the polarization goes to zero along the incident K^- direction, we excluded the events used in the Adair analysis from the Byers-Fenster analysis, thus obtaining two independent results which can be combined, and yield the result that the Ξ^- and Ξ^0 spins are consistent with spin $\frac{1}{2}$, and higher spins are ruled out by ~ 7.2 standard deviations for the Ξ^- and ~ 4.4 standard deviations for the Ξ^0 .

A. Adair analysis

We used only the two-body production channels $K^-p \rightarrow \Xi K$ for this analysis. The z axis was chosen to be along the incident K^- direction; m was the projection of the orbital ΞK angular momentum (l) on this axis. For Ξ production along the z axis, $m=0$.

For $m=0$, the Adair argument uniquely predicts the angular distribution for the decay $\Xi \rightarrow \Lambda \pi$, dependent only on the spin (assuming the usual Λ and π^- spin assignments and unpolarized targets):

$$\text{Spin } J_{\Xi}: \quad P(\alpha): \quad (26)$$

$$\frac{1}{2} \quad 1, \quad (26)$$

$$\frac{3}{2} \quad \frac{1}{2}(1 + 3 \cos^2 \alpha), \quad (27)$$

$$\frac{5}{2} \quad \frac{3}{4}(1 - 2 \cos^2 \alpha + 5 \cos^4 \alpha), \quad (28)$$

$$\infty \quad 1/\sin \alpha, \quad (29)$$

where

$$\cos \alpha = \hat{\Lambda} \cdot \hat{z},$$

$$\hat{z} = K^- \text{ direction, laboratory,}$$

$$\hat{\Lambda} = \Lambda \text{ direction, } \Xi \text{ rest frame.}$$

The decay angular distribution was consistent with an isotropic distribution for all production regions, as required for Ξ spin $= \frac{1}{2}$. For $m=0$ production, this would exclude spin $\frac{3}{2}$. However, as no events occur exactly along the z axis, we must consider how the argument is modified when a finite region near the z axis is used. (The method we used is similar to that of Ref. 10.)

Away from the z axis, $m \neq 0$ is allowed. However, the contribution to the distribution from the $m \neq 0$

terms must go to zero at the z axis, and the rate with which it tends to zero is limited by the maximum angular momentum in the production process. We have therefore estimated the maximum l in the production amplitude, then evaluated the maximum $m \neq 0$ contribution to the Ξ production in a finite region near the z axis. This allowed us to estimate the maximum departure from the distribution of Eqs. (26)–(29) due to the $m \neq 0$ amplitudes.

A fit to the Ξ^- production angular distribution required up to seventh order spherical harmonics for a good fit ($\chi^2 = 35$ for 42 degrees of freedom), and did not improve when higher-order harmonics were added. A maximum angular momentum l allows spherical harmonics of order $2l$ in the intensity. This implies $l=4$ terms are present in the production amplitude (in agreement with the limit obtained from the Adair estimate $l_{\max} = pc/m_\pi$), and suggests that $l=4$ is the maximum angular momentum important in the production amplitude. For the Ξ^0 , the maximum order of spherical harmonics required to fit the production angular distribution was $L=5$, consistent with $l \leq 4$ in the production amplitude. In the following analysis, $l \leq 4$ is assumed for both Ξ^- and Ξ^0 .

It is not possible to determine uniquely the separate contributions of the $m=0$ and $m \neq 0$ terms to the production process from the angular distribution; for example, a $\sin^2\theta$ dependence may result from either an $m \neq 0$ term or from an appropriate combination of the $m=0$ terms giving isotropic and $\cos^2\theta$ dependences. Since the azimuthal variable has been averaged over, there is no way to resolve this ambiguity. However, the maximum $m \neq 0$ contribution can be found.

We fitted the production angular distribution to

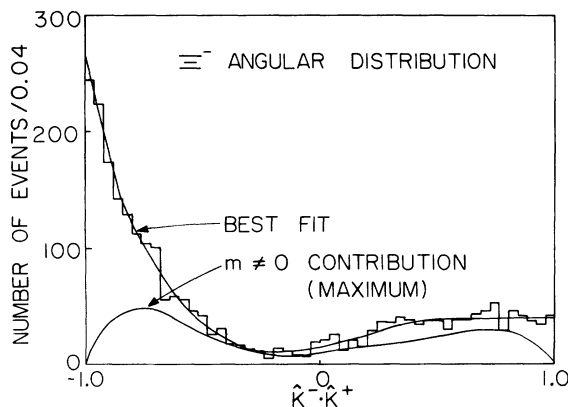


FIG. 18. Fit of the Ξ^- production angular distribution in the reaction $K^- + p \rightarrow \Xi^- + K^+$ to the Legendre polynomials of Eq. (30). The lower curve represents the maximum contribution due to the terms with nonzero projection of the orbital angular momentum on the incident K^- direction.

the set of polynomials

$$f(\theta) = \sum_{K=0}^8 a_K P_K^0(\cos\theta) + \sum_{K=2}^8 b_K P_K^2(\cos\theta) + \sum_{K=4}^8 c_K P_K^4(\cos\theta), \quad (30)$$

where $\cos\theta = \hat{K}^- \cdot \hat{K}^+$ and $P_K^{2m}(\cos\theta)$ = associated Legendre functions. This set of polynomials is not independent. The fit was accomplished by maximizing the $m \neq 0$ contribution (corresponding to the P_K^2 and P_K^4 functions) at the same time that the production distribution was being fitted. Then we forced the fitting program to increase the contribution of the $m \neq 0$ terms contributed beyond that required for the best fit, until the resulting fit was clearly unacceptable (defined as three standard deviations from the best fit). We considered this to be an estimate of the maximum $m \neq 0$ contribution allowed by the data; this contribution is shown in Fig. 18 for the Ξ^- and in Fig. 19 for the Ξ^0 . Notice that the $m \neq 0$ intensity is required to go to zero as $\cos\theta$ goes to ± 1 , so these are regions where $m=0$ production predominates.

For a spin- $\frac{3}{2}$ Ξ , the following decay distributions would be possible (where m_s is the z component of the Ξ spin):

$$m: m_s: P(\alpha): \quad (31)$$

$$0 \quad \pm \frac{1}{2} \quad \frac{1}{2}(1 + 3 \cos^2\alpha), \quad (31)$$

$$\pm 1 \quad \mp \frac{1}{2} \quad \frac{1}{2}(1 + 3 \cos^2\alpha), \quad (32)$$

$$\pm 1 \quad \mp \frac{3}{2} \quad \frac{3}{2} \sin^2\alpha, \quad (33)$$

$$\pm 2 \quad \mp \frac{3}{2} \quad \frac{3}{2} \sin^2\alpha. \quad (34)$$

The relative amounts of these four distributions are determined by the production process. Equal amounts of (31) and (33) would give an isotropic distribution, so to exclude spin $\frac{3}{2}$ we must refer to the Ξ production process to exclude or limit the possible contributions leading to the distributions (33) and (34), i.e., the $m \neq 0$ terms.

Notice that the $m \neq 0$ production could result in either a $\frac{1}{2}(1 + 3 \cos^2\alpha)$ or a $\frac{3}{2} \sin^2\alpha$ decay distribution. We assume the worst case: Let all $m \neq 0$ production result in a $\frac{3}{2} \sin^2\alpha$ distribution. Then the decay angular distribution will have the form

$$P(\alpha) = a(1 + 3 \cos^2\alpha) + b(3 \sin^2\alpha), \quad (35)$$

where a = amount of $m=0$ production and b = amount of $m \neq 0$ production.

From Figs. 18 and 19 we can choose regions where $b < a$ and consider the decay distributions only in those regions. For example, in the Ξ^- production region $1 < \cos\theta < -0.96$, the fit to the production angular distribution limits the $m \neq 0$ contribution to less than 5%. The distribution (35)

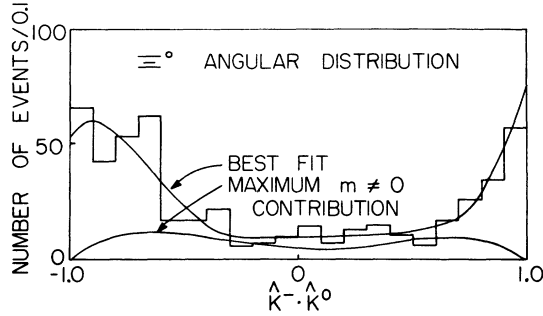


FIG. 19. Fit of the Ξ^0 production angular distribution in the reaction $K^- + p \rightarrow \Xi^0 + K^0$ to the Legendre polynomial of Eq. (30). The lower curve represents the maximum contribution due to the terms with nonzero projection of the orbital angular momentum on the incident K^- direction.

with $b/a = 0.05$ can be compared with the decay angular distribution; it is excluded by 3.3 standard deviations. The production angular distribution for the Ξ^- limits the $m \neq 0$ contribution to be less than the $m = 0$ contribution in the regions $\cos\theta < -0.76$ and $\cos\theta > 0.92$. There are 993 decays in this region, and the total discrimination against spin $\frac{3}{2}$, repeating the above procedure in each bin, is 6.0 standard deviations. For the Ξ^0 , the useful region is < -0.5 and > 0.85 , including 275 decays; this provides a 4.4-standard-deviation discrimination against spin $\frac{3}{2}$ for the Ξ^0 .

For Ξ spins larger than $\frac{3}{2}$, still higher values of m are required to obtain an isotropic distribution.

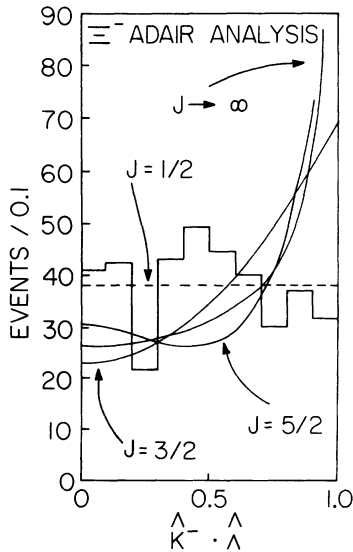


FIG. 20. The Ξ^- decay angular distribution in the reaction $K^- p \rightarrow \Xi^- K^+$ for Ξ^- produced forward ($-1.0 \leq \hat{K}^- \cdot \hat{K}^+ \leq -0.88$), where the $m \neq 0$ contributions are less than 12%. The curves indicate the distributions expected for Ξ^- spins.

Thus spins higher than $\frac{3}{2}$ are ruled out by a number of standard deviations similar to spin $\frac{3}{2}$ for both the Ξ^- and the Ξ^0 .

Figures 20 and 21 show the Ξ^- and Ξ^0 decay angular distributions, with the curves representing the expected distribution for various Ξ spins superimposed. These curves are not the curves of Eqs. (26)–(29); rather, they are the best fit to the decay distribution allowing 12% $m \neq 0$ production, the limit imposed by Figs. 18 and 19 on both these decay regions. The Ξ^0 decay distribution has been folded about $\cos\alpha = 0$; for the Ξ^- , only $\cos\alpha > 0$ events were used because the bias against small kinks affects the $\cos\alpha < 0$ events.

B. Byers-Fenster analysis

A Byers-Fenster-type analysis⁹ was also performed for the Ξ spin. For L odd, the polarization moments are related to the multipole parameters by the following:

Longitudinal polarization moments

$$n_L^J t_L^M = \langle (\vec{P} \cdot \hat{\Lambda}) Y_L^M \rangle; \quad (36)$$

transverse polarization moments

$$n_L^J t_L^M \gamma(2J+1) = \frac{L(L+1)}{(L+\frac{1}{2})^{1/2}} \sum_{L' \text{ even}} \frac{1}{(L+L'+1)^{1/2}} \times \sum_{m=-1}^1 (LM | 1mL'(M-m)) \times \langle P_1^m Y_L^M \tau^m \rangle, \quad (37)$$

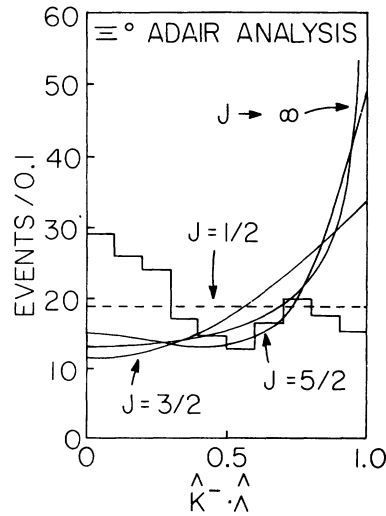


FIG. 21. The Ξ^0 decay angular distribution in the reaction $K^- p \rightarrow \Xi^0 K^0$ for Ξ^0 produced along the K^- direction ($-1.0 \leq \hat{K}^- \cdot \hat{K}^0 \leq -0.84$ and $0.88 \leq \hat{K}^- \cdot \hat{K}^0 \leq 1.0$), where the $m \neq 0$ contributions are less than 15%. The curves indicate the distributions expected for various Ξ^0 spins.

TABLE III. Comparison of results.

α	ϕ (deg)	τ (10^{-10} sec)	Reference
Ξ^- -0.376 ± 0.038	11 ± 9	1.63 ± 0.03	This experiment
-0.391 ± 0.045	-14 ± 11	1.61 ± 0.04	Dauber <i>et al.</i> , Ref. 11
-0.402 ± 0.031	-4.3 ± 8.1	1.660 ± 0.037	Previous world average, Ref. 12
Ξ^0 -0.54 ± 0.10	16 ± 17	$2.88^{+0.21}_{-0.19}$	This experiment
-0.43 ± 0.09	38 ± 19	$3.07^{+0.22}_{-0.26}$	Dauber <i>et al.</i> , Ref. 11
-0.351 ± 0.077	24.8 ± 20.8	$3.03^{+0.18}_{-0.16}$	Previous world average, Ref. 12

where $P_1^0 = P_z$,

$$P_1^{\pm 1} = \mp(P_x \pm iP_y)/\sqrt{2},$$

$$\hat{z} = \hat{K}^- \times \hat{K}^+ / |\hat{K}^- \times \hat{K}^+|, \quad \hat{x} = \hat{K}^-, \quad \hat{y} = \hat{z} \times \hat{x},$$

and γ is the γ_{Ξ} defined by Eq. (8).

By evaluating the right-hand sides of Eqs. (36) and (37) and taking their ratio, $\gamma(2J+1)$ may be measured directly (provided t_L^M is nonzero).

A bias in the data influenced this result. For small kinks in the decay $\Xi^- \rightarrow \Lambda \pi^-$, the scan efficiency suffered. There was a loss of events where the π^- went in the Ξ^- direction. With our choice of coordinate systems, this influenced the M -odd moments, for example, $\text{Re}\langle Y_1^1 \rangle$ was nonzero by 4 standard deviations, but parity conservation in the production process required it to be zero. The correction for the scan loss was made by assuming the requirements of parity conservation were satisfied, so that the lost forward π^- events were the same as the (more efficiently found) backward π^- events in the intervals $|\hat{\pi} \cdot \hat{\Xi}| > 0.7$. The region $\hat{\pi} \cdot \hat{\Xi} > 0.7$ was eliminated, and the region $\hat{\pi} \cdot \hat{\Xi} < 0.7$ was included twice, the second rotated by 180° about the z axis. This corrected the M -odd moments.

After correcting for the bias caused by the small kink loss, there were no moments with $L \geq 2$ that were significantly nonzero, and the requirements of parity conservation in the production reaction were satisfied.

For spin $\frac{1}{2}$, only t_0^0 and t_1^0 can be nonzero. To determine the spin, t_1^0 may be used. This is a measure of the polarization, which varies with production angle, so the right-hand sides of Eqs. (36) and (37) were evaluated separately in each of 10 intervals in the production angular distribution. The ratio of the polarization moments gave a value of $\gamma(2J+1)$ in each interval.

Next, the χ^2 that the two moments were equal was calculated as a function of $\gamma(2J+1)$, using only those intervals not previously used in the Adair analysis. (Excluding those events makes this result independent of the Adair result.) The complete error matrix of the moments was used to account for their correlations. The best value of $\gamma(2J+1)$ was 1.25 ± 0.30 , with a χ^2 of 9.5 for 8 de-

grees of freedom.

If $\gamma = 0.91$ [Eq. (18)], the χ^2 for $J = \frac{1}{2}$ was 11.3; for $J = \frac{3}{2}$, the χ^2 was 28.7. This corresponds to a 3.5-standard-deviation result against spin $\frac{3}{2}$, and excludes higher spins also.

For the Ξ^0 , the result of a similar analysis was not conclusive between $\frac{1}{2}$ and $\frac{3}{2}$.

The result of combining the Adair and Byers-Fenster analyses was the exclusion of spins $\frac{3}{2}$ or higher by 7.2 standard deviations for the Ξ^- and 4.4 standard deviations for the Ξ^0 .

VI. CONCLUSIONS

A. Comparison with previous results

Table III shows our results compared to the most precise previous measurement¹¹ and the current "world average" as given by the Particle Data Group,¹² 1972, which of course does not include the results presented in this paper.

We find the spins of both the Ξ^- and the Ξ^0 to be $\frac{1}{2}$, in agreement with the predictions of SU(3). We can rule out higher spins by 7.2 standard deviations for the Ξ^- and 4.4 standard deviations for the Ξ^0 . Previous to our result, there has been no significant measurement of the Ξ^0 spin, and spins higher than $\frac{1}{2}$ were ruled out by only ~ 3 standard deviations for the Ξ^- .

B. Discussion of results

Parity conservation would require $\alpha = 0$; this is clearly ruled out because both s - and p -wave amplitudes are important in the $\Xi^- \rightarrow \Lambda \pi$ decay.

Time-reversal invariance requires $\beta = 0$, in the absence of final-state interactions. Our results are consistent with that requirement. Including final-state interactions, the requirement on Δ , the phase difference between the $l=0$ and the $l=1$ amplitudes becomes

$$\Delta = \delta_s - \delta_p,$$

where $\tan \Delta = -\beta/\alpha$, and δ_s and δ_p are the $\Lambda \pi$ final-state phase shifts for $l=0$ and $l=1$, respectively.

Since the $\Lambda \pi$ phase shifts are the same for Ξ^- and Ξ^0 decays, T invariance requires $\beta^-/\alpha^- = \beta^0/\alpha^0$ independent of final-state interactions. Our results give $\beta^-/\alpha^- = -0.47 \pm 0.37$ and $\beta^0/\alpha^0 = -0.43 \pm 0.46$, quite consistent with the requirement of T invariance. (The same restriction is imposed by the $|\Delta I| = \frac{1}{2}$ rule, to be discussed below.)

Inverting the argument, if T invariance is assumed, $\delta_s - \delta_p$ can be measured. Using both Ξ^- and Ξ^0 decays together, the result is $\delta_s - \delta_p = (+24^{+13}_{-15})^\circ$.

If CPT is assumed, C invariance would require $\Delta = \delta_s - \delta_p \pm \frac{1}{2}\pi$, or $\delta_s - \delta_p = 114^\circ$ or -66° . Such large

values of the $\Lambda\pi$ phase shifts are unlikely, so this result favors C violation in the Ξ decay.

The $|\Delta I| = \frac{1}{2}$ rule predicts that the decay parameters for Ξ^- and Ξ^0 are the same. From our data, the confidence levels for this are (a) $\alpha_{\Xi^-} = \alpha_{\Xi^0}$, 14% confidence; (b) $\phi_{\Xi^-} = \phi_{\Xi^0}$, 80% confidence.

The $|\Delta I| = \frac{1}{2}$ rule also predicts that $\tau_{\Xi^0} = 2\tau_{\Xi^-}$. Phase space corrections modify this to $\tau_{\Xi^0} = 2.06\tau_{\Xi^-}$; radiative corrections have not been estimated. From our results, the confidence level for $\tau_{\Xi^0} = 2\tau_{\Xi^-}$ is 7%; for $\tau_{\Xi^0} = 2.06\tau_{\Xi^-}$, it is 2.7%, corresponding to a 2.2 standard deviation discrepancy. Thus, while the ϕ parameters are in agreement and the α parameters are in marginal agreement, the lifetimes seem to disagree with the exact $|\Delta I| = \frac{1}{2}$ prediction. The magnitude of the dis-

agreement can be accounted for by a 4% $|\Delta I| = \frac{3}{2}$ amplitude, similar to that required in $K \rightarrow 2\pi$ or in Λ decays, and at the level where electromagnetic corrections may be important.

ACKNOWLEDGMENTS

We would like to thank the scanning and measuring staffs of Columbia University Nevis Laboratories and SUNY at Binghamton for their untiring efforts on this experiment. We also express our thanks to Dr. Hugh Brown and Dr. Horst Foelsche, and the operating crews of the AGS and the 31-in. chamber for their help during the data-taking runs at Brookhaven National Laboratory. We would like to thank Dr. P. Dauber for discussions relevant to the design and analysis of this experiment.

*Research supported by U. S. Atomic Energy Commission and the National Science Foundation.

†Present address: National Science Foundation, Washington, D.C. 20550.

‡Present address: National Center for Atmospheric Research, Boulder, Colorado 80302.

§Present address: Institute for Defense Analysis, Arlington, Virginia 22202.

|| Present address: Brookhaven National Laboratory, Upton, New York 11973.

¹L. K. Gershwin *et al.*, Bull. Am. Phys. Soc. **16**, 569 (1971).

²A. Bridgewater, Columbia University Nevis Report No. 195, 1972 (unpublished).

³C. Baltay *et al.*, Phys. Lett. **42B**, 129 (1972).

⁴M. Habibi, Columbia University Nevis Report No. 199, 1973 (unpublished).

⁵The maximum radius δ ray produced by a 1.75-GeV/c K^- in our magnetic field is 1.9 cm. Larger δ rays result from π^- or μ^- contamination.

⁶For more detail, see Ref. 4.

⁷J. R. Hubbard *et al.*, Phys. Rev. **135**, B183 (1964).

⁸R. Adair, Phys. Rev. **100**, 1540 (1955).

⁹N. Byers and S. Fenster, Phys. Rev. Lett. **11**, 52 (1963).

¹⁰F. Eisler *et al.*, Nuovo Cimento **7**, 222 (1958).

¹¹P. M. Dauber *et al.*, Phys. Rev. **179**, 1262 (1969).

¹²Particle Data Group, Phys. Lett. **39B**, 1 (1972).